Original paper available at:https://doi.org/10.1016/j.enbuild.2018.11.011

Sinusoidal response measurement procedure for the thermal performance assessment of PCM by means of Dynamic Heat Flow Meter Apparatus

Stefano Fantucci[a], Francesco Goia[b*], Marco Perino[a], Valentina Serra[a]

[a] Department of Energy, Politecnico di Torino, Corso Duca degli Abruzzi 24, 10129 Torino, Italy

[b] Department of Architecture and Technology, Faculty of Architecture and Design, NTNU, Norwegian University of Science and Technology, Alfred Getz vei 3, 7491 Trondheim

* Corresponding author: Francesco Goia

E-mail addresses: francesco.goia@ntnu.no

Abstract

The implementation, in Building Performance Simulations (BPS) tools, of robust models capable of simulating the thermophysical behaviour of a Phase Change Material (PCM) represents a fundamental step for an appropriate thermal evaluation of buildings that adopt PCM-enhanced envelope components.

Reliable and robust measuring procedures are essential, at a material and component level, to provide experimental data for the empirical validation of software tools. The traditional laboratory tests that are generally used for the validation of models present some limitations, because PCMs are usually subjected to conditions that may be very different from the real boundary conditions of the building components in which PCMs are applied. Furthermore, in many experimental full-scale mockups, the relatively small quantity of installed PCM and the combination of several thermal phenomena do not allow software tools to be tested in a reliable way.

In this paper, an experimental procedure, based on a modified Heat Flow Meter Apparatus, has been developed to test the behaviour of PCM-enhanced components; the procedure, which is based on the measurement of the sinusoidal response, has been set up to provide data for the comparison and testing of numerical models and of BPS tools. Moreover, general indications and guidelines are provided to solve some issues related to building specimens that contain bulk PCM in order to obtain a more accurate measurement of their performance.//

The experimental results presented in this paper were obtained from two different bulk PCMs (organic and inorganic). It was found that it is important to evaluate different PCM typologies and different thermophysical boundary conditions, including partial and full phase transitions, to test simulation codes that implement PCM modelling functions. In fact, some phenomena, such as hysteresis and subcooling effects are more evident when partial phase transition takes place. The results related to the characterization of the thermal conductivity of a paraffin-based PCM have shown a significant increase (up to 42%) of the equivalent thermal conductivity from a solid to a liquid state, with an upward heat flux, thus highlighting that further investigations and improvements are needed to measure the equivalent thermal conductivity in the different PCM phases.

Keywords: Dynamic heat flow meter, phase change materials, experimental analysis, building components, building energy simulation, model validation.

Acronyms

PCM	Phase Change Material
BPS	Building Performance Simulations
HFM	Heat Flow Meter
DHFM	Dynamic Heat Flow Meter
HVAC	Heating Ventilation and Air Conditioning
PC	Polycarbonate
IC	Initial Conditions
DSC	Differential Scanning Calorimetry

Nomenclature

T	Temperature	°C
ΔT	Temperature difference	°C
R	Thermal resistance	m^2 K W^{-1}
φ	Specific heat flow	W m^{-2}
λ	Thermal conductivity	W m^{-1} K^{-1}
ρ	Density	kg m^{-3}
c_p	Specific heat	kJ kg^{-1} K^{-1}
$c_{p,\,eq}$	Average specific heat over a temperature range	kJ kg^{-1} K^{-1}
e	Thermal effusivity	$J/(s^{1/2}m^2K)$
l	Length	mm
d	Thickness	mm

1. Introduction

In the last few years, thermal energy storage in buildings has grown in popularity, since several challenges, related to energy conservation and building energy management, can be addressed by means of this strategy. On the one hand, the increase in the thermal energy storage capacity of a building is beneficial to reduce the risk of overheating and to improve indoor thermal comfort conditions; on the other hand, important additional benefits can be achieved related to a reduction in the peak energy demand for space heating and cooling. Furthermore, thermal inertia can positively contribute towards reducing the time mismatch between the energy demand profile and the renewable energy availability, thus increasing the rate of renewable energy use in buildings.

In this scenario, Phase Change Materials (PCMs) are considered a promising solution, because of their high thermal energy storage density and their ability to act selectively at different temperature levels (depending on the transition range of the PCM). Nevertheless, in order to obtain a successful use of PCMs in building components, a careful choice of the properties of the material is necessary. The use of Building Performance Simulation (BPS) is in fact crucial to obtain a satisfactory design of PCM-enhanced building components. Although BES software tools, including PCM modelling, have been available for more than a decade, many challenges still exist related to the accurate simulation of PCM-based components, for example, the replication of some particular phenomena, such as hysteresis, sub-cooling and temperature-dependent thermal conductivity.

Reliable and robust measuring procedures are essential, at a material and component level, to provide experimental data for use in the empirical validation of software tools. A widespread dissemination and sharing of experimental datasets is also fundamental.

The aims of the study presented in this paper have been:

i) to develop an experimental procedure for the validation of BPS codes that implement algorithms for the simulation of PCMs. The main goals were to characterise and analyse the thermal behaviour of the bulk-PCM by means of a dynamic heat flow meter apparatus;

ii) to provide thermal properties and experimental data that would allow the BPS results to be compared.

The thermal properties of PCM, related to the latent heat storage capacity, are conventionally measured at a material level in the following ways:

- DSC (Differential Scanning Calorimetry) [1]: this is the most diffused technique and it is based on evaluating the response of a PCM in a series of isothermal steps or a dynamic temperature ramp, both in heating and cooling mode. The main limitation of this technique is that the measurement can only be performed on homogeneous and small sized samples. Moreover, some results may be influenced to a great extent by the test procedure [2] [3]. Furthermore, although the results of enthalpy measurements in heating mode show a good agreement, some discrepancies have been noted in cooling mode measurements (IEA ANNEX 24 - 2011 [4]).
- T-History is an alternative method to DSC to characterize large PCM samples and it can also be used to measure the thermal conductivity of PCMs [5][6]. The method consists in recording the temperature variations during the phase transition and in comparing the results with a well-known reference material, usually distilled water. As previously mentioned, the main advantage, with respect to the DSC method, is that this technique enables the characterisation of large samples and PCM-based building components[7], which are generally non-homogenous.
- DHFM (Dynamic Heat Flow Meter Apparatus):this has recently been introduced in the ASTM C1784:2014 standard [8] and it is a method that can be applied to large-scale specimens (building component scale). The method needs a conventional Heat flow meter apparatus that is generally used for the measurement of thermal conductivity [9][10][11], but it needs to be adjusted to perform dynamic ramp temperature solicitations. The temperature is changed in small steps (as in DSC), and the resulting heat flux that crosses the specimen is measured. The heat capacity is determined as the ratio between the heat flow released or absorbed by the specimen (heat flux variation) and the relative temperature increment [12].

  The main drawback of HFM apparatuses is that they are generally built to host horizontal specimens, and measurements on bulk PCM packed into containers may be affected by uncertainty, due to the volumetric shrinkage of PCM, which leads to the formation of small air pockets in the bulk material.

However, a material characterisation alone is not enough to validate Building Energy Simulation codes (BPS) applied to the analysis of PCM-enhanced building components. Experimental data pertaining to PCM subjected to several partial and total melting/freezing cycles, where the actual operating conditions have been simulated as much as possible, are also necessary [13]. For this reason, several laboratory tests have been carried out in recent years (at a building component scale) with the aim of validating the physical-mathematical models that are implemented in BPS software.

Dynamic measurements, by means of hot-box apparatus, are the most commonly adopted procedures for full-scale mockups [14],[15],[16],[17],[18],[19], and [20]. Nevertheless, most of these experiments have shown some limitations: the PCM specimens were often not thick enough for the change in the slope of the temperature curve to be observed with sufficient accuracy during the phase transition. This happens in particular if the PCM is installed in multilayer components that hide and attenuate the effect of the phase transitions. Moreover, as highlighted in [20], the measurements of some phenomena, such as convection heat transfer, could represent a non-negligible source of uncertainty.

On the other hand, several studies have also been carried out on full-scale components in outdoor test boxes/cells [21],[22] [23],[24],[25],[26],[27],[28] and on roof components [29],[30],[31]. All these studies have provided significant results, since the building components were exposed to the outdoor environment (real conditions) for long periods of time. However, in these cases, not only did the general drawbacks illustrated for the laboratory hot box experiments emerge, but the uncertainties may even have been larger, due to the fact that the specimens were subjected to a multitude of simultaneous dynamic physical phenomena that were not fully controllable.

Although these procedures are usually able to achieve a good empirical validation of numerical models applied to the whole experimental set-up, including the test facility (i.e. the validation is obtained from a comparison of the measured and simulated indoor air temperature), there is, however, a high possibility that one error can compensate another one. In such a case, it becomes difficult to assess the reliability of the part of the code that simulates the PCM heat storage and transfer mechanism separately from the part that solves the full energy balance of the environment. Moreover, the setting up of full-scale laboratory mock-up or the development of in-field experiments implies high costs and requires long-term experimental campaigns, such as in-field experiments.

In order to overcome the shortcomings of the current PCM measurement techniques [32], an experimental procedure has been developed to test the performance of PCM-enhanced building components. This procedure is specifically aimed at providing data for a robust validation of numerical models and of BPS tools that integrate PCM simulation.

2. Measurement methods

Measurements were carried out by means of a modified Heat Flow Meter Apparatus for two different purposes:

- To evaluate the response of PCMs to a sinusoidal temperature difference (dynamic test),
- To measure the thermal conductivity of PCMs during different phases (steady-state conditions).

2.1. DHFM: sinusoidal solicitation response measurements

The use of dynamic measurements, based on sinusoidal tests, offers some advantages over dynamic ramp tests. First, the sinusoidal test method is intrinsically closer to the boundary conditions of a building envelope (i.e. one side of the envelope is considered to remain at a constant temperature, while the other undergoes temperature fluctuations that can be described through a series of sinusoidal functions). Second, such an approach allows a comparison to be made with the equivalent dynamic response (time lag and decrement factor) presented in the, EN ISO standard 13786:2007 method [33] (Thermal performance of building components - Dynamic thermal characteristics - Calculation methods). It is worth mentioning that a direct application of the EN ISO 13786 standard to building envelope components, making use of PCMs, is not possible. In fact, this technical standard applies to materials that are characterised by linear behaviour (that is, their thermophysical properties do not vary with the temperature). Nevertheless, the principle behind this standard can be applied, with suitable modifications, to the case of PCMs, and useful information can be derived.

Heat Flow Meter apparatus (HFM) is primarily used to determine the thermal properties of a material under a steady-state heat flux (thermal conductivity or thermal resistance) [10],[11]. The system is generally composed of a heating/cooling unit, heat flow meters and temperature sensors (thermocouples) placed on the surfaces of a specimen (upper and lower plates). The measurement principle is based on the generation of a constant temperature difference between the two sides of a specimen, and on the measurement of the heat flux density. Heat flow sensors and thermocouples are generally positioned in a relatively small area, compared to the total area of the heated/cooled plates, with the aim of measuring the physical quantities over an area that is not affected by edge effects. The main components of the HFM apparatus and its working principle are illustrated in Figure 1.

----------Figure 1----------

As previously mentioned, traditional HFM apparatuses are designed to work under steady state boundary conditions (e.g. ΔT constant over time). Nevertheless, DHFM (Dynamic Heat Flow Meter) apparatuses have recently been developed. These are essentially an HFM apparatus with more advanced software and a control unit that is able to reproduce the time-varying boundary conditions. These instruments make it possible to execute:

i) temperature ramps;
ii) sinusoidal periodic temperature variations.

and can be used for different purposes:

i) to measure the specific volumetric heat and enthalpy according to ASTM C1784 [8]. The principle is based on the measurement of the amount of heat absorbed/released by the specimen which, starting from an initial condition of equilibrium (steady state temperature field), is then subjected to a temperature variation. Tests are generally repeated over a series of temperature ranges. Some examples of these tests are shown in [1],[12] and [34];
ii) to measure the response of a specimen exposed to a sinusoidal temperature variation on one side (solicited side). The analysis is generally performed by measuring the response, in terms of time profiles of the heat flux density on the side exposed to a constant temperature. Some examples of these tests are reported in [3] and [35].

The second approach has been used in the present study, since sinusoidal solicitations are more realistic for validating the capability of BPS codes to properly simulate the actual behaviour of building envelope components that make use of PCMs.

2.2. Thermal conductivity measurement of the bulk PCM – Data analysis procedure

The thermal conductivity of the two PCM substances was also measured by means of the heat flow meter apparatus described in section 2.1.1, according to the procedure described in EN 12664:2002 [11]. The characterisation was carried out on polycarbonate panels filled with PCM (section 3.2), sandwiched between two thin rubber mats (2 mm thick) instead of gypsum boards. This material was selected because it allows the contact resistance to be reduced and the measurement accuracy to be increased (the additional thermal resistance of the rubber mats is significantly lower than that of a gypsum board)

Since the specimens were constituted by different layers and materials, it was not possible to directly evaluate the thermal conductivity of just the bulk PCM. An indirect determination was therefore carried out. The equivalent thermal conductivity of the bulk PCM was assessed as the total resistance of the specimen, measured by the HFM devices, less the thermal resistance of the rubber sheets (previously measured) and the calculated thermal resistance of the polycarbonate layers (eq. 1):

$$R_{PCM} = R_{spec.} - R_R - R_{PC} \quad (1)$$

where: R_{PCM} is the thermal resistance of the bulk PCM, R_R is the thermal resistance of the two rubber sheets, R_{PC} is the thermal resistance of the two polycarbonate layers (upper PCM side and lower PCM side) and $R_{spec.}$ is the total thermal resistance of the multilayer specimen. This last quantity, for in-series resistance, is equal to the ratio between the temperature difference ΔT, measured in the upper and lower plates (T_{up} and T_{low}), and the measured heat flux density (eq. 2).

$$R_{spec.} = \frac{\Delta T}{\varphi} \quad (2)$$

The thermal resistance of the two polycarbonate layers (upper and lower sides), R_{PC}, was determined by means of eq. (3), assuming a thermal conductivity, $\lambda_{PC,}$ of 0.205±0.015 W/mK (as reported in the literature [36]), while the polycarbonate thickness d_{PC} was measured by means of a Vernier caliper (instrumental resolution of 0.02 mm).

$$R_{PC} = \frac{2 \cdot d_{PC}}{\lambda_{PC}} \quad (3)$$

The PCM thermal conductivity λ_{PCM} resulted to be:

$$\lambda_{PCM} = \frac{d_{tot} - 2 \cdot d_{Rubber} - 2 \cdot d_{PC}}{R_{PCM}} \quad (4)$$

The thermal conductivity of the two PCM substances was also measured in two modes, i.e. with an upward and with a downward heat flux. The reason for this procedure is to ensure that the results were independent of the flux direction (especially when the material was in the liquid phase) – or, if a dependence of the result on the flux direction emerged, in order to explain such behaviour.

3. Materials and specimens

3.1. Materials

An experimental campaign was carried on two commercially available PCM substances (PCM-a) and (PCM-b), which are representative of two different types of PCM: PCM-a is an organic paraffin (commercial name: RT 28 HC); PCM-b is an inorganic salt hydrate (commercial name: SP 26 E). The two PCMs were selected because they are characterised by different hysteresis behaviour (which is higher in PCM-b) and because they represent two typical products used for building envelope components. The most relevant thermophysical properties of the two PCM substances are shown in Table 1 (more detailed information can be found in [37]), while the physical properties of the materials that constitute the multilayer experimental specimens are summarized in Table 2 [13] and Figure 2 [37]. The PCM was macro-encapsulated in a polycarbonate alveolar structure (as described in the next sections).

----------Table 1----------

199 ----------Figure 2----------

200 ----------Table 2----------

201 ### 3.2. Specimens preparation

202 Most of the studies reported in the literature that make use of HFM apparatuses were mainly focused on PCM composite
203 systems (e.g. PCM-gypsum boards, PCM-plasters and shape stabilized PCM in a polymeric matrix) and only a few of
204 them considered the properties of bulk PCM. Moreover, whenever these properties were studied, attention was usually
205 focused on the solid phase and the melting/solidifying process was neglected [38].

206 One of the reasons for the lack of characterisations of bulk materials is the difficulties encountered in performing the
207 measurements in a heat flow meter apparatus. In particular, when the PCM is not incorporated in a composite system, and
208 is instead enclosed in a container, several issues that affect the measurements may arise, that is:

209 - Difficulty in sealing the specimen (resulting in PCM leakage and loss of material);
210 - Volumetric thermal expansion of the PCM, which prevents the container from being filled completely (formation
211 of air gaps);
212 - The presence of thermal bridges, which can affect the results (metallic containers);
213 - Convection phenomena in the liquid phase (when the PCM is enclosed in a relatively large cavity).

214 A new approach has been developed to perform experimental investigations on bulk PCM by means of DHFM apparatus
215 in order to overcome the above-mentioned issues. Such an approach is based on the use of alveolar polycarbonate
216 containers (Figure 3), a system that presents several advantages over more conventional metallic containers. First, the
217 thermal properties of polycarbonates are of the same order of magnitude as those of PCMs (the thermal conductivity of
218 polycarbonate ranges between 0.19 – 0.22 W/mK, with a density of ~ 1200kg/m^3 [36]), and therefore limit the potential
219 thermal bridge effects induced by the polycarbonate structure. Second, the alveolar structure (9x9 mm cells) reduces the
220 convective phenomena when the PCM is liquid. In order to solve the issue of the volumetric expansion of the PCM, the
221 two open sides of the specimens were bent to create an expansion volume that was then filled with PCM when its
222 volumetric density decreases due to the liquid phase state. Such a strategy prevents the formation of air gaps within the
223 measurement area.

224 ----------Figure 3----------

225 A comparison of the procedure commonly (Fig. 4a) adopted in previous studies ([31], [38] and [39]) and the one (Fig.
226 4b) adopted in this study is presented in Figure 4. The advantages of the proposed strategy, compared to the conventional
227 one, can be summarised as:

228 - measurements can be conducted without sealing the PCM container (sealing issues and PCM leakage problems
229 are resolved);
230 - the entire volume in the specimen can be completely filled by liquid PCM, thus avoiding the occurrence of air
231 bubbles;
232 - the excess of PCM in the expansion volume compensates for the shrinkage of the PCM during the solidification
233 process, so that the specimen is always and completely filled with PCM to its upper surface.

234 ----------Figure 4----------

3.3. Experimental test rig and procedure

The PCM-polycarbonate experimental specimens were sandwiched between two gypsum board panels (Figure 5). The primary reason for the insertion of the two gypsum boards is due to measurement constraints: without any additional "insulation" layer in the test sample, the measured heat flux (μV) could exceed the upper limit of the HFM signals (overflow). Such an event can occur, especially during the phase transition of the PCM, when a high amount of energy is stored/released over a short time interval. The upper limit of the HFM signal may be increased by changing the setting of the HFM user interface, but such a procedure has an adverse effect of increasing the acquisition time-step, which results in a significant reduction in the number of measurement points, and it is therefore not recommended.

The second reason for the selected layout for the test specimen is that the adoption of gypsum boards allows the temperature in the upper and lower interfaces of a PCM-polycarbonate layer to be measured by means of external sensors and these temperatures to be decoupleds from the influence of the HFM plates, which are maintained at controlled temperatures (Figure 6). Type-E thermocouples (nominal accuracy ±0.25°C), calibrated in the laboratory, were positioned between the gypsum board and the PCM specimen (two thermocouples). One thermocouple was placed in the centre of the PCM layer (Figure 7), with a dedicated ring surrounding the probe (acting as a spacer) to ensure that the temperature values were acquired at the centre of the PCM-polycarbonate specimen.

----------Figure 5----------

----------Figure 6----------

----------Figure 7----------

The Heat Flow Meter Apparatus used in the experiment was a Lasercomp FOX600 single sample device, modified to perform dynamic experiments. The device allows a 24h periodic sinusoidal temperature variation to be imposed in one of the two plates, while the other plate is kept at a constant temperature. The experiments lasted 48h (2 x 24 h cycle), and only the results of the second cycle were stored as dynamic equilibrium was reached in the second measurement cycle (stabilised 24h harmonic state). Before starting the measurement of the two cycles, an initialization period was necessary, and the dynamic cycles were not started before the setpoint temperature had been reached in both of the instrument plates. Two different tests (*test 1* and *test 2*) were carried out, imposing a lower plate temperature equal to the nominal melting temperature of the PCM, and an upper sinusoidal temperature with different amplitudes, that is, 28±12°C (PCM-a) and 26±12°C (PCM-b) (total phase transition) for *test 1,* and 28±6 °C (PCM-a) and 26 ±6 °C (PCM-b) (partial phase transition) for *test 2,* respectively (Figure 8). The reason two different tests were performed with different temperature amplitudes on one of the two plates was to define one cycle (T_{upper} ± 12°C) where the entire latent heat of the PCM system was exploited (i.e. when the system completely underwent two phase change cycles, from solid to liquid state, and back to the original solid) and another cycle (T_{upper} ± 6°C) where the entire latent heat was not exploited – and therefore the PCM system could not complete the phase change.

----------Figure 8----------

4. Preliminary numerical verification

Numerical heat transfer analyses were carried out to verify the following assumptions:

- The stabilisation of the 24h periodic regime: to verify that two sinusoidal cycles of 24h each were sufficient to achieve a 24h periodic regime.
- The hypothesis of mono-dimensional heat transfer: to verify that the alveolar geometry of the polycarbonate would not determine any significant deviation from the 1D heat flux.

The numerical analyses were carried out using WUFI®2D [40], [41]. This is a well-known software that has been validated for two-dimensional, transient heat and moisture transfer purposes.

In this software, building components containing PCM can be simulated by assigning an enthalpy vs temperature curve as input data.

4.1. Verification of measurement initialisation

A numerical analysis was carried out with the aim of verifying that two sinusoidal cycles of 24h each (and thus a total duration of the test of 48h) are sufficient to achieve the stabilization of the harmonic state, when the initial conditions are in a range of temperatures that is near the phase change temperature range.

For this reason, two sinusoidal cycles were simulated, starting from three different initial conditions (IC) of the temperature of the PCM layer: 30°C (PCM in the liquid phase), 28°C (PCM in the melting phase) and 26°C (solid phase). The results are shown in Figure 9. As it is possible to observe, the same value of the temperature of the PCM layer is reached after ~6h for all the simulations. Nevertheless, in order to take into account that the simulation software might not have been completely accurate (hysteresis phenomena and sub-cooling phenomena were not implemented), the results of the first 24h were discarded (to be on the safe side), and only the results obtained during the second cycle (from 24th and 48th hours) were used for the analysis.

----------Figure 9----------

4.2. Verification of a mono-dimensional heat flow assumption

The subsequent analysis was aimed at verifying that the effect of the vertical polycarbonate (PC) structures that connected the upper and lower panel was negligible when the heat transfer across the PCM layer was assessed. This assumption allowed the polycarbonate-PCM system to be simplified and to be considered as a structure of layers (PC+PCM+PC). The heat transfer for this geometry was mono-dimensional.

A 2D transient simulation was performed for this verification. In order to reduce the computational costs of the simulation, the geometry of the problem was simplified considering only a small portion of the specimen (30mm width) constituted by three cavities filled with PCM (a representative "module" of the entire structure of the sample under test).

The temperature values of four "sensor" points (two for each side of the PCM layer) were compared to verify the negligibility of the 2D heat transfer. The four sensors were placed in the middle of the PCM cell and in proximity of the vertical bridges of the polycarbonate, as shown in Figure 10. If the maximum temperature difference between the central sensors (T1) and the sensors located on the sides (T2) were lower than the measurement accuracy of the thermocouples (±0.25 °C), the 2D heat transfer phenomena, due to the vertical bridges in the polycarbonate container, could be neglected (because, in practice, it is not measurable).

----------Figure 10----------

306 The difference between the central temperature sensor (T1) and the temperature sensors located on the sides (T2) is shown
307 in Figure 10. The results show a maximum difference of 0.040 °C and 0.013 °C for the lower side and the upper side of
308 the PCM layer, respectively, with associated root mean square errors, RMSE (between the central point and the side
309 point) of about 0.003 and 0.002 °C. These figures confirm that it is possible to neglect the 2D heat transfer phenomena,
310 as a result of the shape and the thermophysical properties of the polycarbonate.

311 ----------Figure 11----------

312 **5. Results and discussion**

313 **5.1. Thermal conductivity results**

314 The results of the thermal conductivity measurements are shown in Table 3. Even though these results are affected by a
315 rather high uncertainty, due to the use of an indirect assessment method (see section 2.2) and the consequent error
316 propagation, it is possible to observe that the following points.

317 • The thermal conductivity of PCM-a (organic - paraffin wax) is, as expected, dependent on the PCM state. When
318 the measurement is carried out at an average temperature of 20 C (solid state), the thermal conductivity, λ, is
319 found to be in the 0.28 to 0.29 W/mK range (a coherent value with those reported in the $\lambda_{declared}$ datasheet), and
320 independent of the heat flow direction. Conversely, when the measurement is carried out at 35 °C (liquid state),
321 the thermal conductivity, λ, assumes very different values, depending on the flow direction. When the test is
322 carried out with a downward flow, the thermal conductivity decreases to 0.15 W/mK; when tested with an
323 upward flow, it increases to 0.41 W/mK. This difference can be justified considering the development of
324 naturally-induced convective heat transfer phenomena when the PCM is in liquid phase (despite the small size
325 of the cavities). In the case of the downward flux, these natural convective phenomena are suppressed because
326 of the direction of the heat transfer, while they are enhanced in the case of an upward flux. Therefore, in the
327 latter case, this measured value should be interpreted as an equivalent thermal conductivity value that includes
328 both convection and conduction. However, the determined equivalent thermal conductivity value is only valid
329 for the presented configuration (boundary conditions and geometry). Other configurations could lead to
330 differences in the flow patterns, which would lead to different equivalent thermal conductivity values.
331 Convection is usually neglected in PCM models, not only in those for BPS tools, but also in specifically
332 developed models. However, the results of experiments show how these phenomena may play a non-negligible
333 role, depending on the configuration of the envelope component, and on the nature of the PCM. In order to
334 account for the coupled convection-conduction heat transfer in thin PCM layers, the equivalent thermal
335 conductivity λ_{eq} value may be used for both characterisation and modelling purposes. Unfortunately, because of
336 the measurement set up, it was not possible to measure the equivalent thermal conductivity for horizontal thermal
337 gradients (i.e. in the case of an element installed in a wall). However, an investigation on these convective heat
338 exchanges in small alveolar structures, in the case of different heat flux directions, could provide more insight
339 into the relevance of the convective heat transfer.
340 • PCM-b (inorganic – salt hydrate) also presents a variable value of λ_{eq} for the two different phases. In the solid
341 phase, the equivalent thermal conductivity is in the 0.59 W/mK range, in line with the value found in the material
342 datasheet, and it is quite insensitive to the flux direction – as expected. When in the liquid phase, the thermal
343 conductivity decreases to values in the 0.45 to 0.46 W/mK range, depending on the flux direction. However, in
344 this case, the difference in the value of the equivalent thermal conductivity that may be induced by the flux

direction is very small, and well within the measurement uncertainty threshold value. These results lead to the hypothesis that the presence of a salt matrix in PCM-b suppresses the buoyancy effects, or limits them to a great extent, and consequently the convective heat exchange when the material is in a liquid state.

----------Table 3----------

5.2. Sinusoidal solicitation response analysis

The results of the four experimental test, two for each PCM substance, carried out by means of the DHFM apparatus, are plotted in Figures 12 and 13.

----------Figure 12----------

----------Figure 13----------

It is possible to observe that all the results are consistent with those reported in the literature regarding the behaviour of the two different PCM compositions [37], and in particular:

- In Test 1 (PCM-a and b), the change in the slope (PCM temperatures), due to the total melting and solidification of the PCM, is evident, while the change is much less evident in Test 2 with a sinusoidal amplitude of 6°C, thus leading to the hypothesis that the PCM remains in its "mushy" state without completing the phase transition. The complete melting/solidification process can be seen in Test-1, as changes in the slope of the temperature profile can be observed at around time ~13 (nucleation of test 1 a) and time ~17 (end of the solidification phase in test 1 a). On the other hand, the two different PCMs in Test 2 lead to different results. While PCM-b always remains within the phase transition range, it can be seen, in Fig. 13 (Test-2), that the entire latent heat of fusion is exploited, and that the PCM is in a liquid state between time-step ~8 and time-step ~16. However, the system cannot complete the subsequent solidification process, and remains in its mushy state from time-step ~16 to time-step ~8.

  The reason for this different behaviour of the two PCMs may be explained considering the different thermal conductivities of the materials, rather than the different specific latent heat capacities. In fact, even though the paraffin-based PCM (PCM-a) has a specific latent heat capacity of ~216 kJ/kg (temperature range 26-29°C), which is ~40 % higher than that of the salt hydrate PCM (which is equal to ~153 kJ/kg in the 23-26°C temperature range), the density of the two materials also differs to a great extent: ~825 kg/m^3 and ~1450 kg/m^3, for PCM-a and PCM-b, respectively. The combination of these properties leads to volumetric latent heat capacities of ~178200 kJ/m^3 (temperature range 26-29°C) and ~221850 kJ/m^3 (temperature range 23-26°C), for PCM-a and PCM-b, respectively.

  On the other hand, the two PCMs present very different thermal conductivities (that of the salt hydrate is larger than that of the paraffin-based PCM). This feature leads to equivalent thermal effusivities e_{eq} (eq. 5) for the phase transition range (26-29°C for PCM-a and 23-26°C for PCM-b) of ~3023 J/s$^{1/2}$m^{2}K and of ~5853 J/s$^{1/2}$m^{2}K for PCM-a and PCM-b, respectively. A comparison of these two values can help support the hypothesis that, in the case of PCM-a, and under Test-2 conditions, the overall properties of the system lead to the full exploitation of the latent heat of fusion, while this does not occur in the case of PCM-b.

$$e_{eq} = \sqrt{\lambda \cdot \rho \cdot c_{p,eq}} \quad (5)$$

where the equivalent thermal capacity $c_{p,eq}$ [kJ/kg K] in the phase change temperature range is obtained by dividing the specific latent heat capacity [kJ/kg] by the temperature range of the transition [K].

- The sub-cooling effect is clearly visible in all the tests. Nevertheless, it should be underlined that this effect is more evident in Test 1 (complete phase transition) and in PCM-a (organic - paraffin wax).
- Salt hydrate PCM-b shows a more evident hysteresis effect (~1.5-2 °C of difference between the melting and the congealing temperature) in both Test 1 and Test 2, compared to the paraffin PCM. In the latter material, the hysteresis phenomenon is of limited significance, in general terms, but becomes particularly negligible when thermal stress occurs with very slow heating/cooling rates (lower than 0.04 ºC/min).

The temperature values plotted in Fig. 12 and Fig. 13 are reported in Table 4, with a time-step of 30 minutes, in appendix A. The full set of experimental data containing a shorter time-step resolution, the temperatures and heat flow measured at the boundary conditions (plates), as well as the temperature values at the different interfaces of the samples are reported so that they can be used for comparisons with software codes. Observing the relevant difference in the PCM behaviour, according to the type of solicitation (12 ºC amplitude or 6 ºC amplitude), it is recommended that numerical models should be tested against both of the tests presented in this paper. This is necessary to ensurethat the comparison process, between numerical and experimental results, covers a wide range of thermal conditions (which are more representative of the actual building operating conditions in which partial and total transition can occur), and not only the situation in which a PCM completes both the heating and the cooling phases. Moreover, it is advisable to and include phenomena such as sub-cooling and hysteresis, which might not be negligible, depending on the type of PCM substance (organic-inorganic), in the simulation models.

6. Conclusion

An experimental procedure, set up to assess the thermal behaviour of PCMs in real building components, on the basis of sinusoidal response measurements with DHFM apparatus, is presented in this paper.

In order to measure the thermal performance of PCM layers under sinusoidal solicitations, a set of preliminary numerical analyses was carried out before the experimental activity. The obtained results show that the polycarbonate container used to encapsulate the bulk PCM substances had a negligible effect on the heat transfer phenomena (no generation of 2D temperature fields). Two sinusoidal cycles (48h) proved to be sufficient to accurately measure the PCM behaviour, since the thermal fields were found to be independent of the initial conditions after the first cycle (24h).

As far as the influence of the PCM type and state on the global heat transmission is concerned, the results demonstrate that, for PCM-a (solid phase) and PCM-b (both phases), the thermal conductivity is slightly different from that reported in literature, but with no significant changes between upward/downward heat fluxes (natural convection phenomena can be considered suppressed). On the other hand, the results for PCM-a in a liquid state can Can be somewhat different from the thermal conductivity literature data, especially for an upward heat flux, which may be significantly higher due to the occurrence of convection heat transfer phenomena.

For this reason, more precise measurements of the equivalent thermal conductivity for bulk-PCM contained in several kinds of structures should be performed in order to obtain accurate simulation input data.

The experimental sinusoidal response measurements on PCM substances highlight that it is important to evaluate different boundary conditions for the testing of simulation codes that implement PCM modelling capabilities. The following guidelines should be followed:

- The results on PCM-a (paraffin wax PCM), with a complete phase transition (test 1), should be used to verify the reliability of a simulation code that implements a sub-cooling effect;
- The results on PCM-b (salt hydrate PCM), for both test 1 (complete transition) and test 2 (partial transition), should be used to validate models that implement the hysteresis phenomena;
- The thermal conductivity of PCM-b also changes significantly during a phase change. Therefore, it may be used to test simulation codes that consider temperature dependent thermal conductivity;
- Test 2, on both PCM-a and PCM-b, may be used to test numerical codes that simulate building components that implement PCMs under the actual thermal conditions of a building (partial transition can frequently occur). Test 1 (PCM-a and b) is only useful to estimate the capability of simulation codes to simulate the total phase transition of PCM;
- The test on PCM-a (paraffin wax PCM) can be used for comparison purposes with codes that implement the temperature-dependent thermal conductivity of PCM substances.

7. Acknowledgments

The authors would like to express their gratitude to Alice Lorenzati, Rocco Costantino, and Maurizio Bressan for their helpful support during the experimental activities. A part of the research activities presented in this paper was carried out in the framework of a Short Term Scientific Mission (STSM), supported by the European Union COST Action TU1403 (Adaptive Facades Network). The authors also gratefully acknowledge COST Action TU1403 for providing the excellent scientific network.

References

[1] ASTM E793 - 06(2012 Standard Test Method for Enthalpies of Fusion and Crystallization by Differential Scanning Calorimetry

[2] Kosny, Jan; Stovall, Therese K; Yarbrough, David W. Dynamic Heat Flow Measurements to Study the Distribution of Phase-Change Material in an Insulation Matrix. 30th International Thermal Conductivity Conference, Seven Springs, PA, USA, (2009)

[3] Cascone Y., Perino M., Estimation of the thermal properties of PCMs through inverse modelling. Energy procedia, 78 (2015), 1714 – 1719. https://doi.org/10.1016/j.egypro.2015.11.275

[4] IEA (2011) Development of a test-standard for PCM and TCM characterization part 1: characterization of phase change materials. Technical report. IEA—Solar Heating and Cooling/ Energy Conservation through Energy Storage programme—Task 42/Annex 24: Compact Thermal Energy Storage: Material Development for System Integration. http://www.iea-eces. org/files/a4.3.a2_appendix_wga2_1.pdf

[5] Zhang YP, Jiang Y, Jiang Y. A simple method, the T-history method, of determining the heat of fusion, specific heat and thermal conductivity of phase-change materials. Measur Sci Technol 1999;10:201-5. DOI 10.1088/0957-0233/10/3/015

[6] Marín JM, Zalba B, Cabeza LF, Mehling H. Determination of enthalpy-temperature curves of phase change materials with the temperature history method: improvement to temperature dependent properties. Measur Sci Technol 2003;14:184-189. DOI 10.1088/0957-0233/14/2/305

[7] Kosny, Jan, PCM-enhanced building components, An Application of Phase Change Materials in Building Envelopes and Internal Structures. Springer (2015). DOI 10.1007/978-3-319-14286-9.

[8] ASTM C1784:2014, Standard Test Method for Using a Heat Flow Meter Apparatus for Measuring Thermal Storage Properties of Phase Change Materials and Products.

[9] ASTM C518:2010, Standard Test Method for Steady-State Thermal Transmission Properties by Means of the Heat Flow Meter Apparatus

[10] EN ISO 12667:2001, Thermal performance of building materials and products - Determination of thermal resistance by means of guarded hot plate and heat flow meter methods - Products of high and medium thermal resistance

[11] UNI EN 12664:2001, Thermal performance of building materials and products - Determination of thermal resistance by means of guarded hot plate and heat flow meter methods- Dry and moist products of medium and low thermal resistance

[12] Shukla N., Kosny J. DHFMA Method for Dynamic Thermal Property Measurement of PCM-integrated Building Materials. Curr Sustainable Renewable Energy Rep (2015) 2:41–46. DOI 10.1007/s40518-015-0025-x

[13] Goia F, Chaudhary G, Fantucci S. Modelling and experimental validation of an algorithm for simulation of hysteresis effects in phase change materials for building components, Energy and Buildings 174 (2018), 54-67. https://doi.org/10.1016/j.enbuild.2018.06.001

[14] Cao S, Gustavsen A, Uvsløkk S, Jelle BP, Gilbert J, Maunuksela J. The effect of wall-integrated phase change material panels on the indoor air and wall temperature - hot box experiments. In: Proceedings of renewable energy research conference (2010), Trondheim, Norway, 7–8 June

[15] Haavi, T, Gustavsen A, Cao S, Uvsløkk S, Jelle B.P. Numerical Simulations of a Well-Insulated Wall Assembly with Integrated Phase Change Material Panels - Comparison with Hot Box Experiments," The International Conference on Sustainable Systems and the Environment (2011), Sharjah, United Arab Emirates.

[16] Kossecka E., Kosny, J., "Hot-Box Testing of Building Envelope Assemblies—A Simplified Procedure for Estimation of Minimum Time of the Test," Journal of Testing and Evaluation, Vol. 36, No. 3, 2008, pp. 242-249, https://doi.org/10.1520/JTE100795. ISSN 0090-3973

[17] Kośny J, Yarbrough DW, Miller W, Childs P, Syed AM (2007b) Thermal performance of PCM-enhanced building envelope systems. In: Proceedings of X conference - thermal performance of the exterior envelopes of buildings (2007), Clearwater, Florida.

[18] Kuznik F, Virgone J, Noel J. Optimization of a phase change material wallboard for building use. Appl Therm Eng 28 (2007), 1291–1298. https://doi.org/10.1016/j.applthermaleng.2007.10.012

[19] Kuznik F, Virgone J, Experimental investigation of wallboard containing phase change material: Data for validation of numerical modeling, Energy and Buildings 41 (2009), 561-570, https://doi.org/10.1016/j.enbuild.2008.11.022

[20] Kuznik F, Virgone J, Johannes K., Development and validation of a new TRNSYS type for the simulation of external building walls containing PCM. Energy Build 42 (2010), 1004–1009. https://doi.org/10.1016/j.enbuild.2010.01.012

[21] Medina MA, Stewart R. Phase-change frame walls (PCFWs) for peak demand reduction, load shifting, energy conservation and comfort. In: Proceedings of Sixteenth symposium on improving building systems in hot and humid climates (2008), Plano, TX.

[22] Medina MA, Zhu D. A comparative heat transfer examination of structural insulated panels (SIPs) with and without phase change materials (PCMs) using a dynamic wall simulator. In: Proceedings of Sixteenth symposium on improving building systems in hot and humid climates (2008), Plano, TX.

[23] Khudhair AM, Farid MM. Use of phase change materials for thermal comfort and electrical energy peak load shifting: experimental investigations. In: Goswami DY, Zhao Y (eds) Solar world congress 2007. Solar Energy and Human Settlement (2007), Beijing, China.

[24] Tardieu A, Behzadi S, Chen J, Farid M., Computer simulation and experimental measurements for and experimental PCM-impregnated office building. In: Proceedings of building simulation 2011: 12th conference of international building performance simulation association (2011), Sydney.

[25] Cabeza L, Castellon C, Nogues M, Medrano M, Leppers R, Zubillaga O. Use of microencapsulated PCM in concrete walls for energy savings. Energy Build 39 (2007), 113–119. https://doi.org/10.1016/j.enbuild.2006.03.030

[26] Castell A, Medrano M, Castellón C, Cabeza LF. Analysis of the simulation models for the use of PCM in buildings. In: Proceedings of Effstock 2009 - the 11th international conference on thermal energy storage (2009), Stockholm, Sweden.

[27] Castell A, Martorell I, Medrano M., Pérez G, Cabeza L.F. Experimental study of using PCM in brick constructive solutions for passive cooling, Energy and Buildings 42 (2010), 534–540. https://doi.org/10.1016/j.enbuild.2009.10.022

[28] Castellón C, Medrano M, Roca J, Cabeza L, Navarro M, Fernández A, Lázaro A, Zalba B. Effect of microencapsulated phase change material in sandwich panels. Renew Energy 35 (2010), 2370–2374. https://doi.org/10.1016/j.renene.2010.03.030

[29] Miller WA, Karagiozis A, Kośny J, Shrestha S, Christian J, Kohler C. Demonstration of four different residential envelopes. In: Proceedings of ACEEE Summer study on energy efficiency in building (2010), Pacific Grove, California.

[30] Kośny J, Miller W, Zaltash A Dynamic thermally disconnected building envelopes—a new paradigm for walls and roofs in low energy buildings. In: Proceedings of DOE, ASHRAE, ORNL Conference—thermal envelopes XI—thermal performance of the exterior envelopes of buildings (2010), Clearwater, Florida.

[31] Elarga H, Fantucci S, Serra V, Zecchin R, Benini E. Experimental and numerical analyses on thermal performance of different typologies of PCMs integrated in the roof space, Energy and Buildings (2017), https://doi.org/10.1016/j.enbuild.2017.06.038.

[32] Dutil Y, Rousse D, Lassue S, Zalewski L, Joulin A, Virgone J, Kuznik F, Johannes K, Dumas J.P, Bédécarrats J.P, Castell A, Cabeza L. F. Modeling phase change materials behavior in building applications: Comments on material characterization and model validation, Renewable Energy 61 (2014), 132-135. https://doi.org/10.1016/j.renene.2012.10.027

[33] EN ISO 13786:2007. Thermal performance of building components - Dynamic thermal characteristics - Calculation methods.

[34] Ruuska T, Vinha J, Kivioja H. Measuring thermal conductivity and specific heat capacity values of inhomogeneous materials with a heat flow meter apparatus, Journal of Building Engineering, 9 (2017), 135-141, https://doi.org/10.1016/j.jobe.2016.11.011

[35] Carbonaro C, Cascone Y, Fantucci S, Serra V, Perino M, Dutto M. Energy Assessment of a PCM-Embedded Plaster: Embodied Energy Versus Operational Energy, Energy Procedia, 78 (2015), 3210-3215, http://dx.doi.org/10.1016/j.egypro.2015.11.782

[36] Incropera F. P, DeWitt D. P. Fundamentals of Heat and Mass Transfer, 3rd ed. Wiley (1990).

[37] https://www.rubitherm.eu/en/productCategories.html <accessed 21.05.2017>

[38] Bianco L, Serra V, Vigna I, Energy assessment of a novel dynamic PCMs based solar shading: results from an experimental campaign, Energy and Buildings (2017), https://doi.org/10.1016/j.enbuild.2017.05.067.

[39] Komerska A, Bianco L, Serra V, Fantucci S, Rosiński M. Experimental Analysis of an External Dynamic Solar Shading Integrating PCMs: First Results, Energy Procedia, 78 (2015), 3452-3457, http://dx.doi.org/10.1016/j.egypro.2015.11.125

[40] IBP, WUFI® 2D version 3, Fraunhofer Institute for Building Physics, Holzkirchen, Germany, https://wufi.de/en/software/wufi-2d/_ (14 May 2017).

[41] Künzel H M 1995. Simultaneous Heat and Moisture Transport in Building Components, Fraunhofer IRB Verlag Stuttgart, Germany. ISBN 3-8167-4103-7

[42] CEI ENV 13005:2000. Guide to the expression of uncertainty in measurement, (2000).

[43] S. Fantucci, F. Goia, M. Perino, V. Serra, Dynamic temperature profiles in a poly-carbonate panel filled with phase change materials under test in a Dynamic Heat Flow Meter Apparatus, Mendeley Data, v1 (2018), http://dx.doi.org/10.17632/ygxk82g498.1

Appendix A

Table 4. Dataset. 2nd measurement cycle (24 – 48 h), more detailed experimental results (DHFM heat fluxes and temperatures with a time step of 666 seconds) are available on the following link: http://dx.doi.org/10.17632/ygxk82g498.1[43].

	PCM-a (paraffin wax)						PCM-b (salt-hydrate)					
	Test 1 (12 ºC amplitude sinusoidal solicitation)			Test 2 (6 ºC amplitude sinusoidal solicitation)			Test 1 (12 ºC amplitude sinusoidal solicitation)			Test 2 (6 ºC amplitude sinusoidal solicitation)		
time	$T_{PCM, core}$	$T_{PCM, up}$	$T_{PCM, low}$	$T_{PCM, core}$	$T_{PCM, up}$	$T_{PCM, low}$	$T_{PCM, core}$	$T_{PCM, up}$	$T_{PCM, low}$	$T_{PCM, core}$	$T_{PCM, up}$	$T_{PCM, low}$
s	ºC	ºC	ºC	ºC	ºC	ºC	ºC	ºC	ºC	ºC	ºC	ºC
0	26.0	26.2	26.4	26.4	26.5	26.6	24.2	24.4	24.4	24.3	24.4	24.5
1800	26.5	26.9	26.7	26.6	26.9	26.7	24.6	25.0	24.6	24.6	24.8	24.7
3600	26.9	27.5	27.0	26.8	27.2	26.8	25.0	25.6	25.0	24.8	25.1	24.9
5400	27.2	28.1	27.2	26.9	27.4	26.9	25.4	26.2	25.4	25.0	25.4	25.1
7200	27.4	28.5	27.3	27.1	27.7	27.0	25.7	26.7	25.6	25.3	25.7	25.3
9000	27.5	29.1	27.4	27.3	28.0	27.1	26.0	27.2	25.8	25.5	26.0	25.4
10800	27.7	29.8	27.5	27.4	28.2	27.2	26.2	27.8	26.0	25.7	26.2	25.5
12600	28.0	30.5	27.5	27.5	28.4	27.2	26.5	28.3	26.1	25.8	26.5	25.6
14400	28.6	31.3	27.6	27.6	28.6	27.3	27.0	29.0	26.8	25.9	26.6	25.7
16200	29.0	32.1	27.7	27.9	28.9	27.3	29.3	31.0	28.7	26.0	26.8	25.7
18000	29.6	32.8	27.8	28.1	29.2	27.3	30.3	31.9	29.6	26.0	26.9	25.8
19800	31.3	33.8	29.1	28.4	29.5	27.4	30.7	32.3	30.0	26.2	27.0	25.8
21600	33.0	35.3	30.9	28.6	29.6	27.4	31.0	32.4	30.1	26.4	27.2	26.0
23400	33.3	35.6	31.2	28.8	29.8	27.5	30.9	32.3	30.1	26.7	27.5	26.4
25200	33.3	35.5	31.2	28.9	29.9	27.5	30.7	32.1	29.9	27.3	28.0	26.9
27000	33.2	35.3	31.1	28.9	29.9	27.6	30.5	31.8	29.7	27.6	28.2	27.1
28800	32.9	34.9	31.0	29.0	29.9	27.6	30.2	31.4	29.5	27.8	28.3	27.3
30600	32.6	34.4	30.7	29.1	30.0	28.2	29.8	30.8	29.2	27.7	28.2	27.2
32400	32.1	33.7	30.5	29.3	30.0	28.5	29.3	30.1	28.7	27.5	27.9	27.1
34200	31.5	32.9	30.1	29.2	29.8	28.5	28.7	29.4	28.3	27.2	27.6	26.9
36000	30.9	32.1	29.7	29.0	29.4	28.3	28.1	28.6	27.8	26.9	27.3	26.7
37800	30.2	31.1	29.3	28.7	29.0	28.1	27.5	27.8	27.2	26.7	26.9	26.4
39600	29.6	30.2	28.8	28.2	28.5	27.9	26.8	26.9	26.6	26.3	26.5	26.1
41400	28.7	29.1	28.3	27.8	28.0	27.6	26.0	25.9	26.0	25.9	26.1	25.8
43200	27.9	28.0	27.8	27.3	27.4	27.3	25.3	25.0	25.4	25.5	25.6	25.5
45000	27.2	26.9	27.3	26.9	26.9	27.1	24.6	24.2	24.9	25.1	25.2	25.2
46800	27.7	27.3	27.7	27.5	27.3	27.5	24.0	23.3	24.3	24.7	24.7	24.9
48600	27.7	26.9	27.7	27.5	27.2	27.5	23.9	22.6	23.9	24.3	24.3	24.6
50400	27.7	26.4	27.7	27.4	27.0	27.5	24.1	23.0	24.5	23.9	23.8	24.3
52200	27.5	26.0	27.7	27.3	26.8	27.5	24.2	23.0	24.6	23.6	23.4	24.0
54000	27.2	25.5	27.7	27.2	26.6	27.6	24.2	22.9	24.7	23.7	23.3	23.9
55800	26.8	24.9	27.6	27.0	26.4	27.5	24.1	22.6	24.6	23.8	23.3	23.9
57600	26.4	24.3	27.5	26.8	26.2	27.5	23.9	22.3	24.5	24.0	23.3	24.0
59400	25.8	23.5	27.0	26.7	26.0	27.5	23.6	22.0	24.1	23.9	23.2	24.1
61200	24.6	22.4	25.7	26.4	25.7	27.4	23.0	21.3	23.3	23.8	23.1	24.1
63000	22.6	20.7	24.1	26.2	25.5	27.4	22.0	20.5	22.5	23.5	23.1	24.1
64800	21.5	19.8	23.3	25.9	25.2	27.2	21.2	19.7	21.8	23.5	23.1	24.2
66600	21.2	19.5	23.1	25.6	24.9	26.9	20.6	19.2	21.3	23.4	23.1	24.2
68400	21.2	19.6	23.1	25.3	24.6	26.4	20.3	19.0	21.0	23.4	23.1	24.2
70200	21.4	19.9	23.2	24.9	24.3	25.9	20.4	19.1	21.0	23.4	23.1	24.2
72000	21.7	20.2	23.4	24.6	24.1	25.6	20.5	19.4	21.1	23.4	23.1	24.2
73800	22.0	20.7	23.6	24.5	24.1	25.5	20.8	19.9	21.4	23.4	23.2	24.2
75600	22.5	21.3	23.9	24.7	24.3	25.5	21.2	20.4	21.8	23.4	23.2	24.1
77400	22.9	22.0	24.3	24.9	24.6	25.6	21.7	21.0	22.2	23.4	23.2	23.9
79200	23.5	22.7	24.7	25.1	24.9	25.8	22.3	21.8	22.7	23.4	23.3	23.9
81000	24.2	23.5	25.1	25.4	25.3	26.0	22.8	22.5	23.1	23.5	23.4	23.9
82800	24.8	24.4	25.5	25.7	25.7	26.2	23.2	23.1	23.5	23.7	23.7	24.0
84600	25.3	25.1	25.9	26.0	26.0	26.3	23.5	23.6	23.9	23.8	23.9	24.2

555

List of figures with correspondent captions

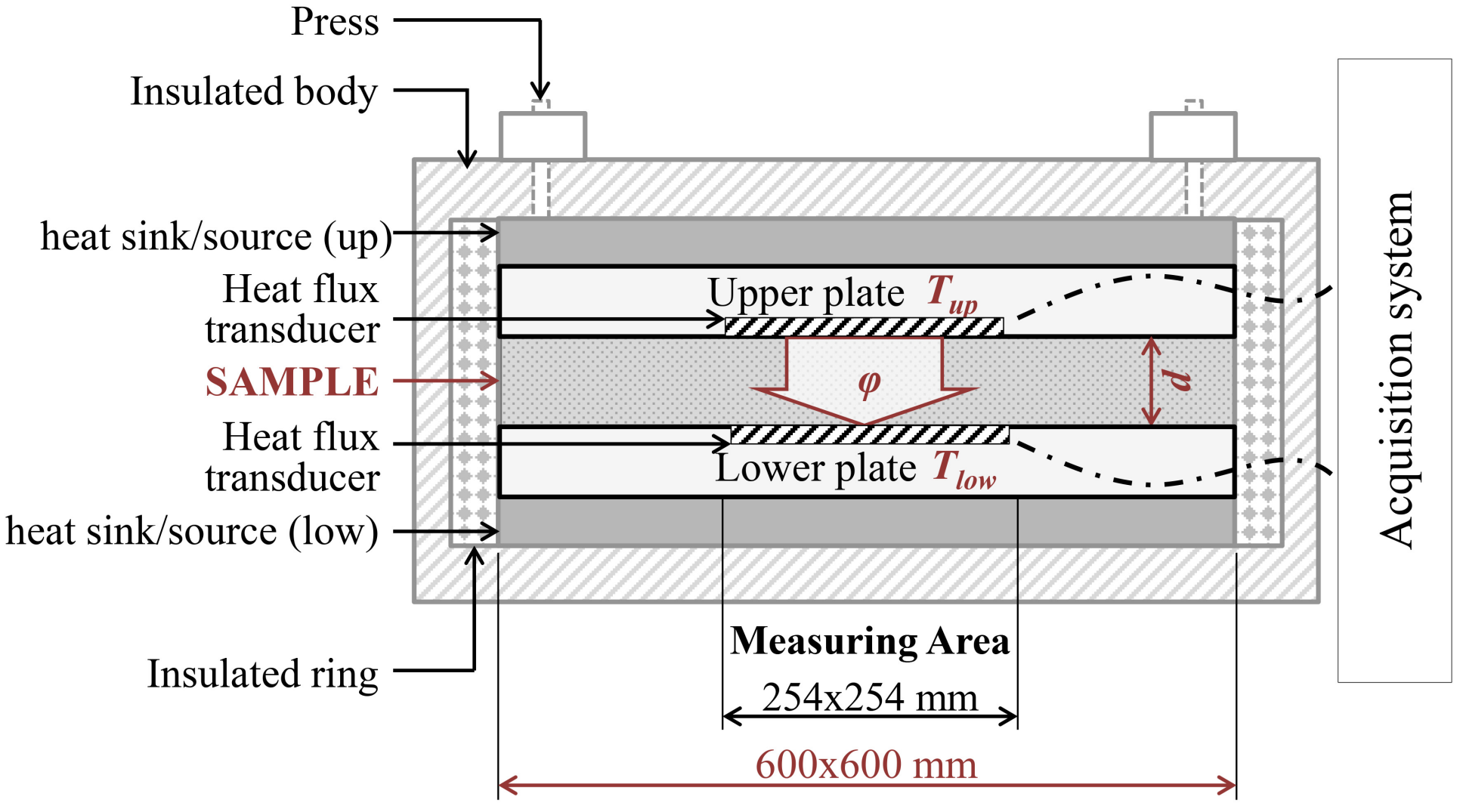
Press
Insulated body
heat sink/source (up)
Heat flux transducer
SAMPLE
Heat flux transducer
heat sink/source (low)
Insulated ring
Upper plate T_{up}
φ
d
Lower plate T_{low}
Measuring Area
254x254 mm
600x600 mm
Acquisition system

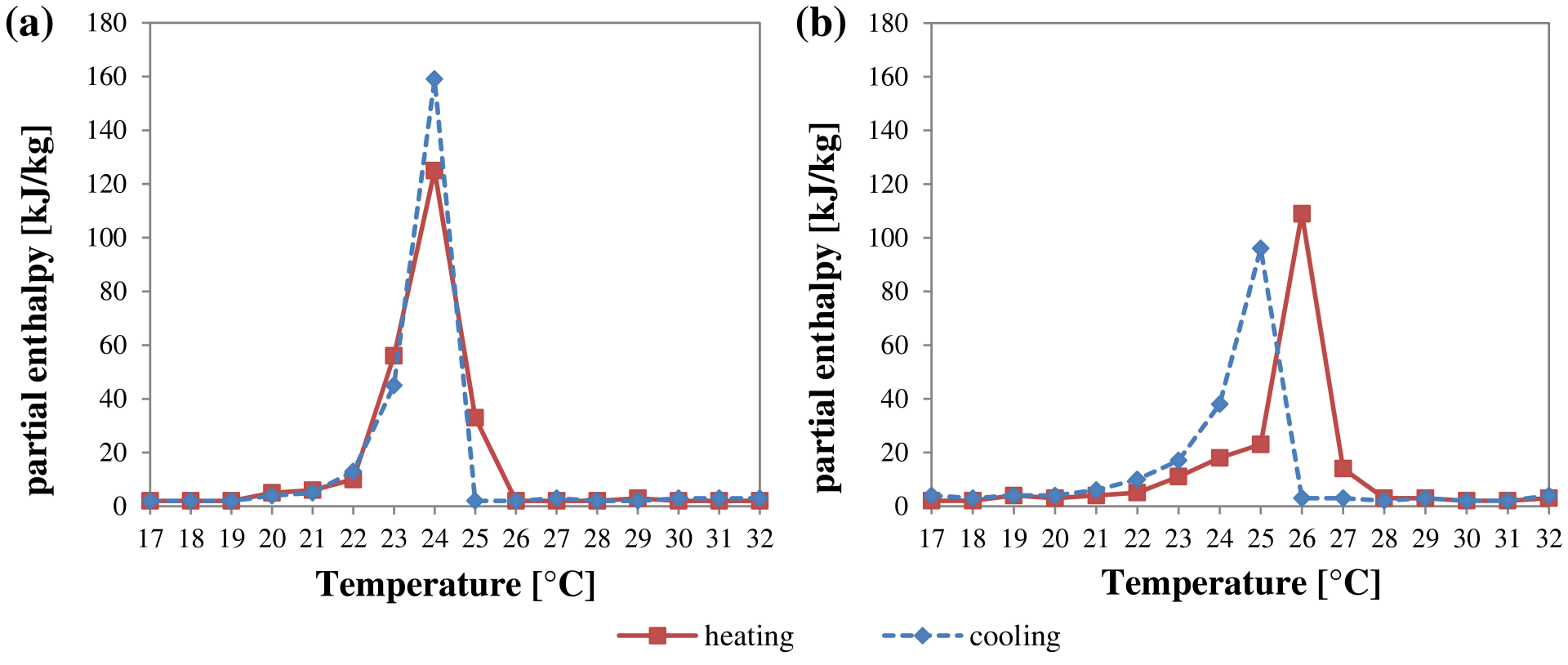
(a)
(b)
partial enthalpy [kJ/kg]
0
20
40
60
80
100
120
140
160
180
17 18 19 20 21 22 23 24 25 26 27 28 29 30 31 32
Temperature [°C]
heating
cooling

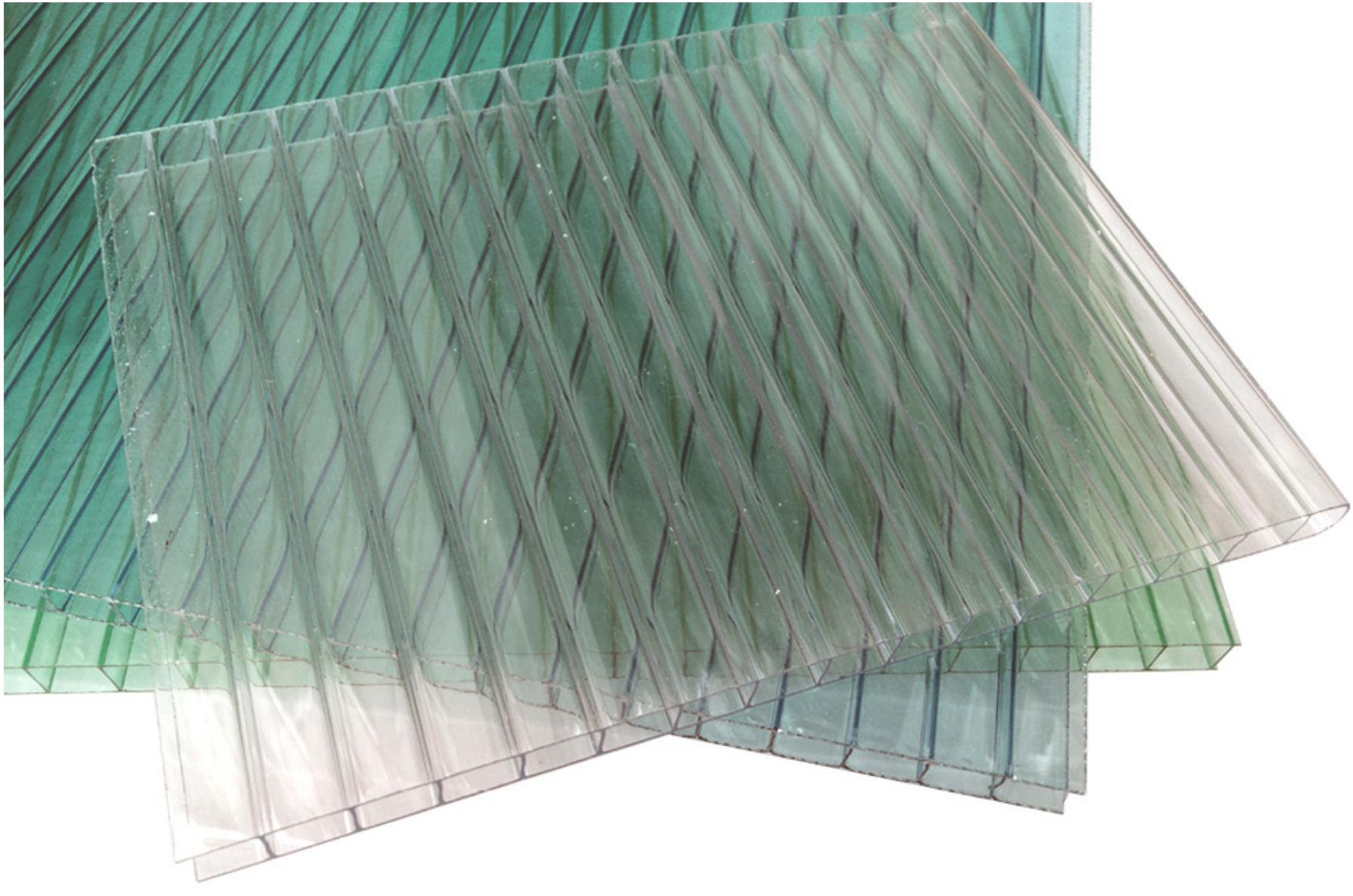

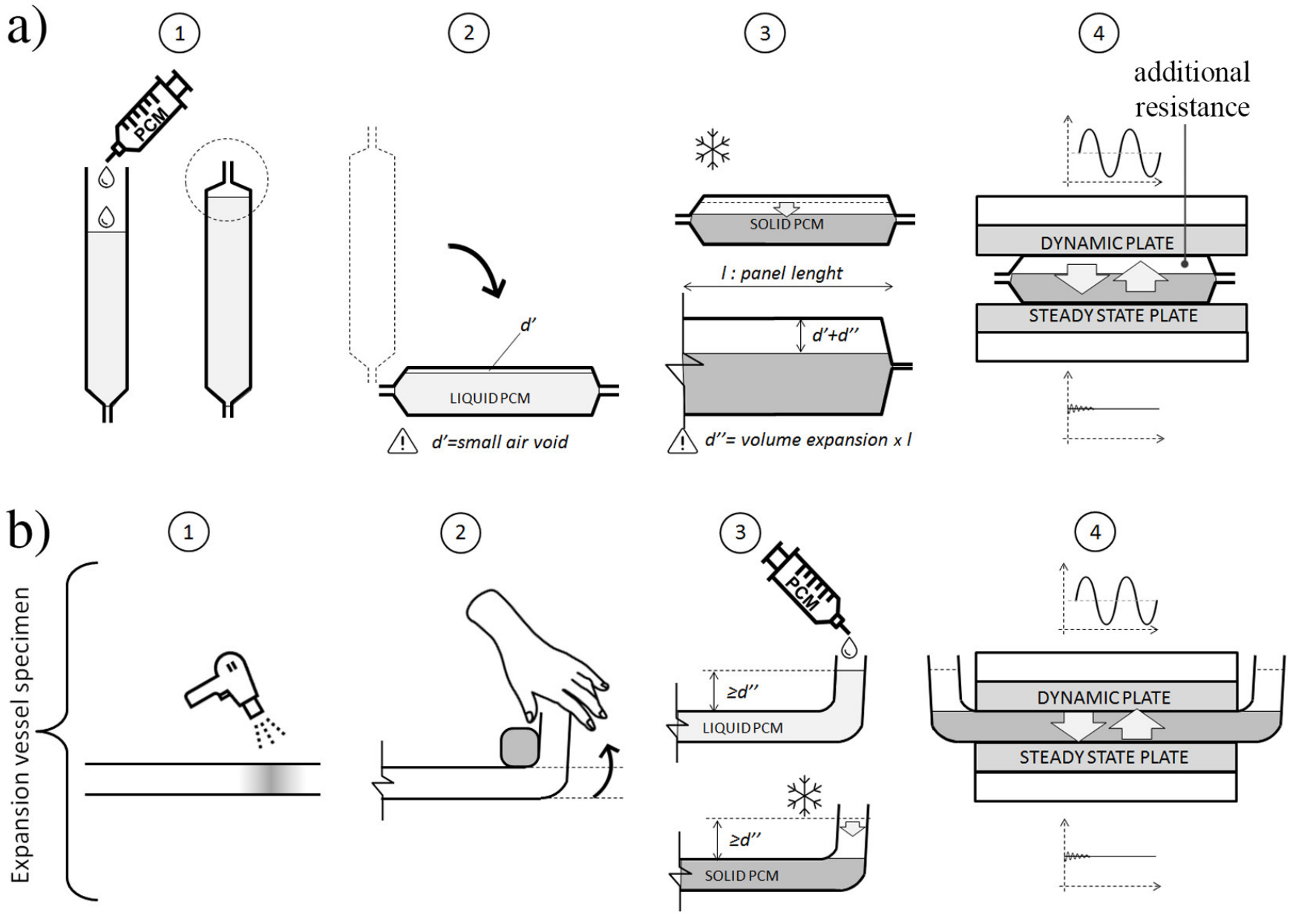
a)
1
2
3
4
PCM
d'
LIQUID PCM
d'=small air void
SOLID PCM
l : panel lenght
d'+d''
d''= volume expansion x l
additional
resistance
DYNAMIC PLATE
STEADY STATE PLATE
b)
1
2
3
4
Expansion vessel specimen
PCM
≥d''
LIQUID PCM
≥d''
SOLID PCM
DYNAMIC PLATE
STEADY STATE PLATE

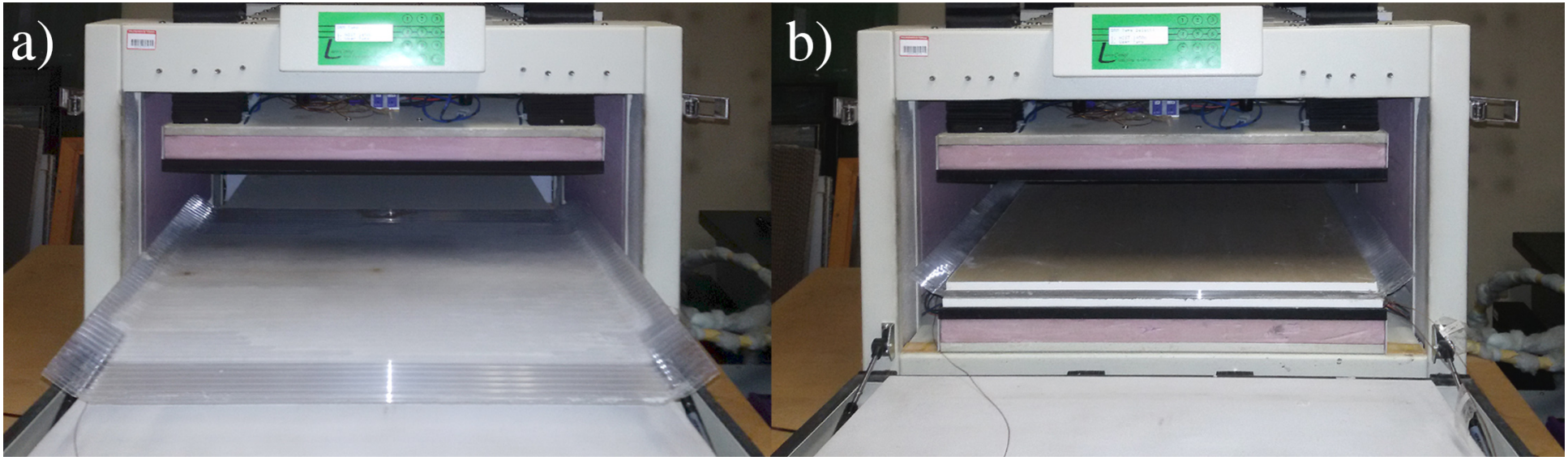
a)
b)

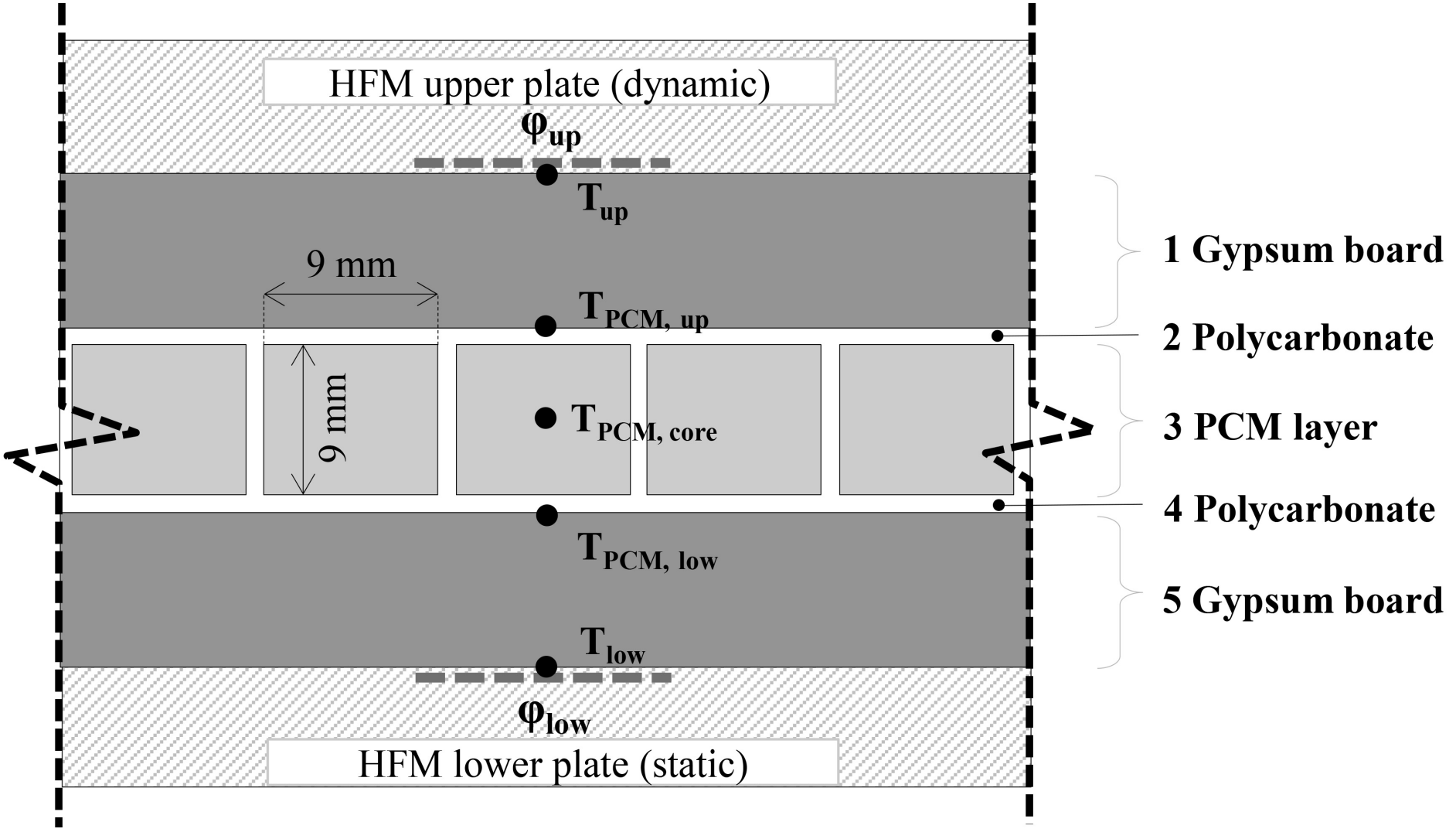
HFM upper plate (dynamic)
φup
Tup
9 mm
TPCM, up
9 mm
TPCM, core
TPCM, low
Tlow
φlow
HFM lower plate (static)
1 Gypsum board
2 Polycarbonate
3 PCM layer
4 Polycarbonate
5 Gypsum board

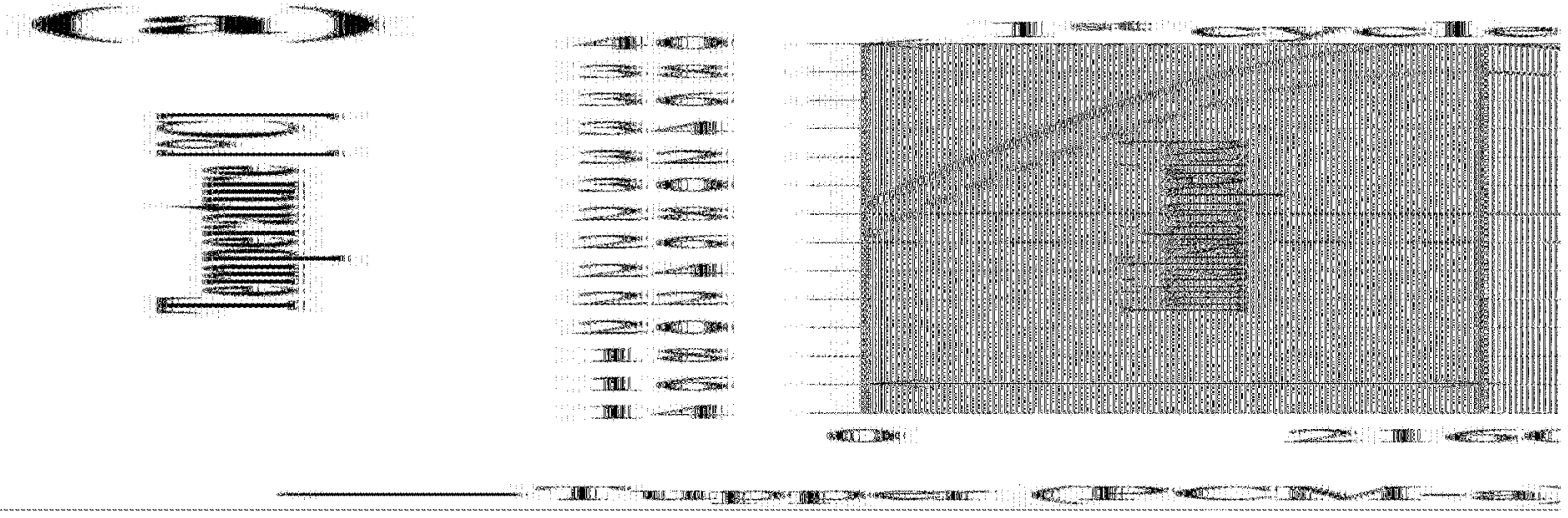

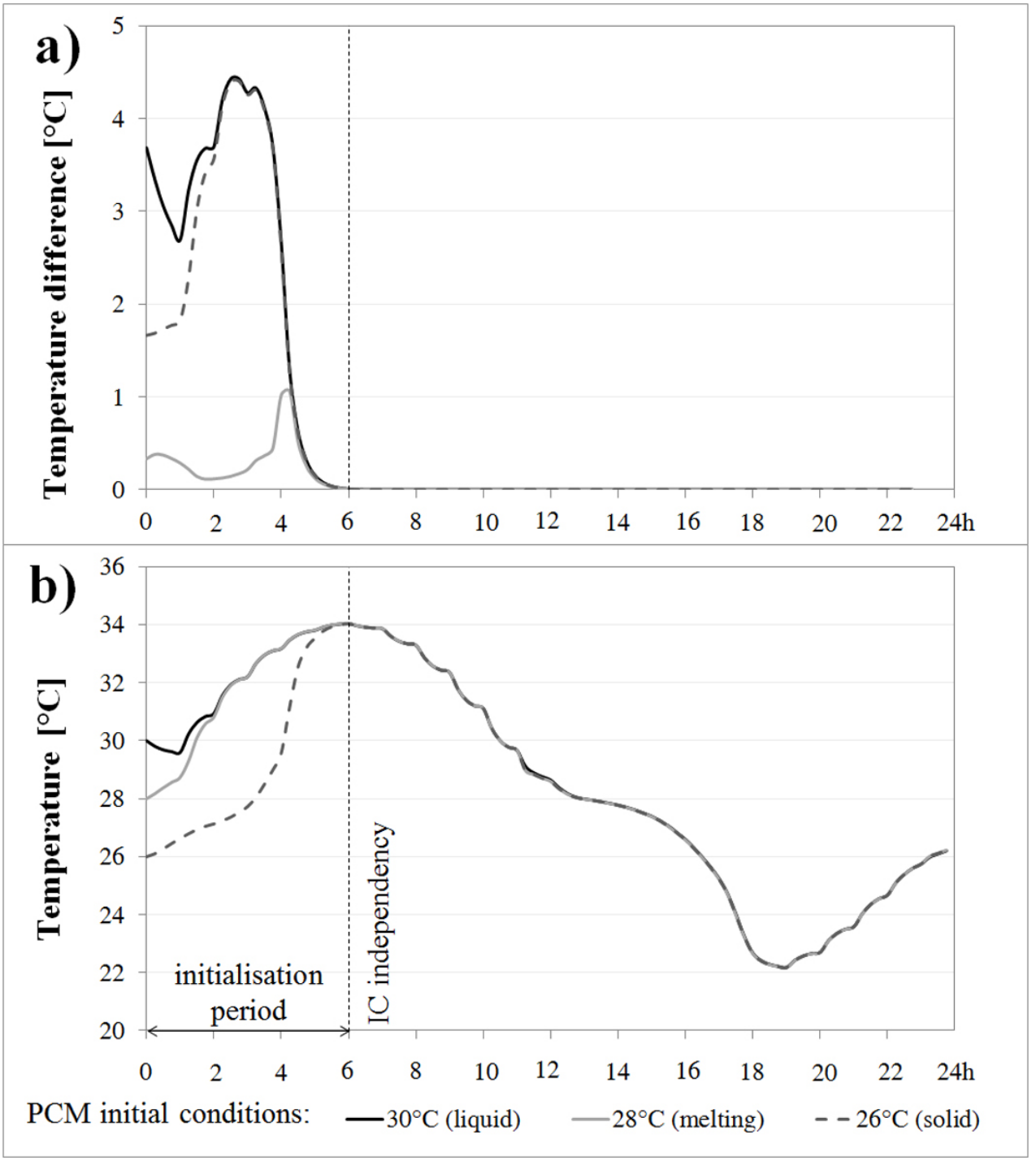
a)
Temperature difference [°C]
5
4
3
2
1
0
0
2
4
6
8
10
12
14
16
18
20
22
24h
b)
Temperature [°C]
36
34
32
30
28
26
24
22
20
initialisation period
IC independency
0
2
4
6
8
10
12
14
16
18
20
22
24h
PCM initial conditions:
30°C (liquid)
28°C (melting)
26°C (solid)

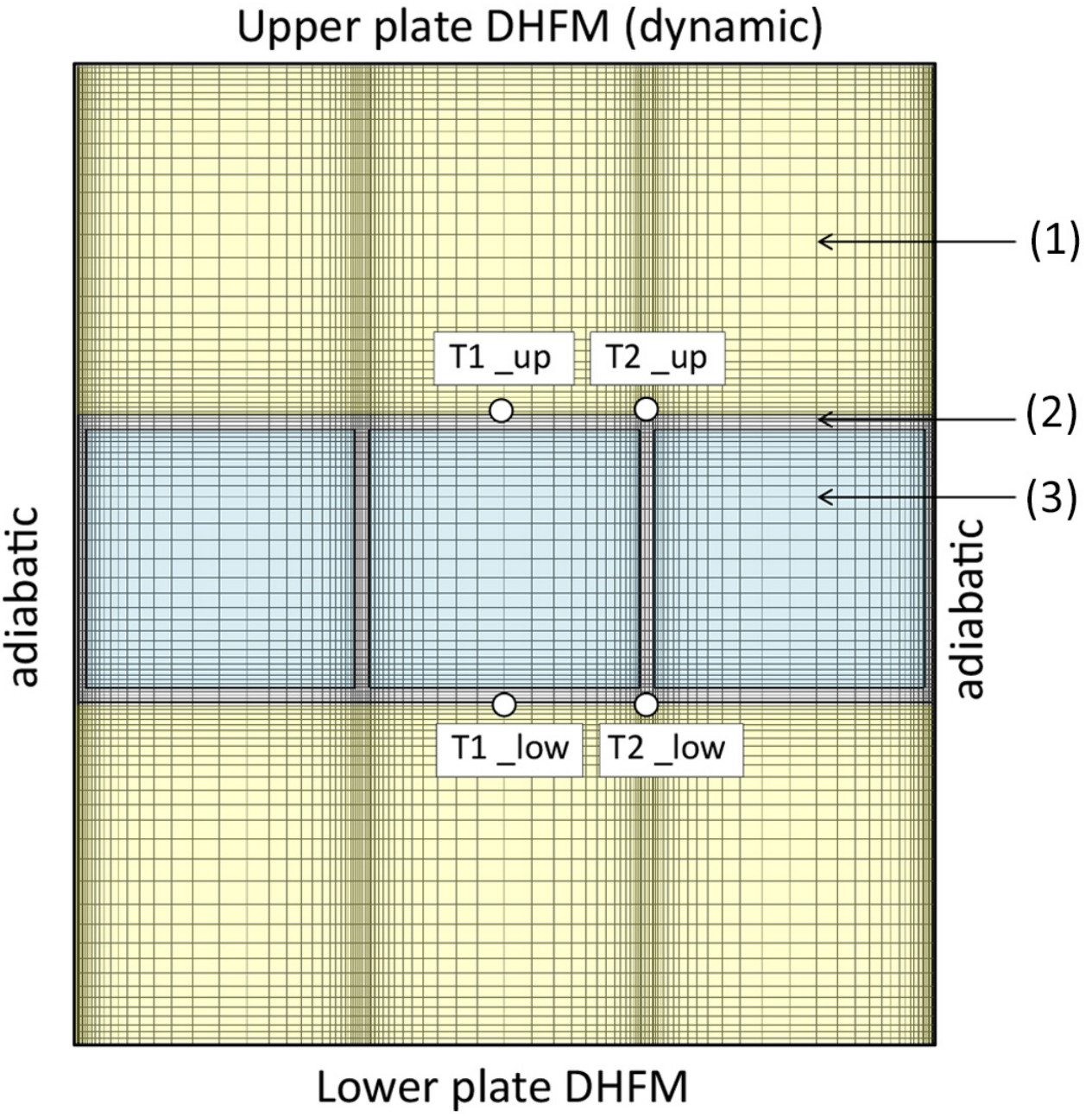
Upper plate DHFM (dynamic)
(1)
T1 _up
T2 _up
(2)
(3)
adiabatic
adiabatic
T1 _low
T2 _low
Lower plate DHFM

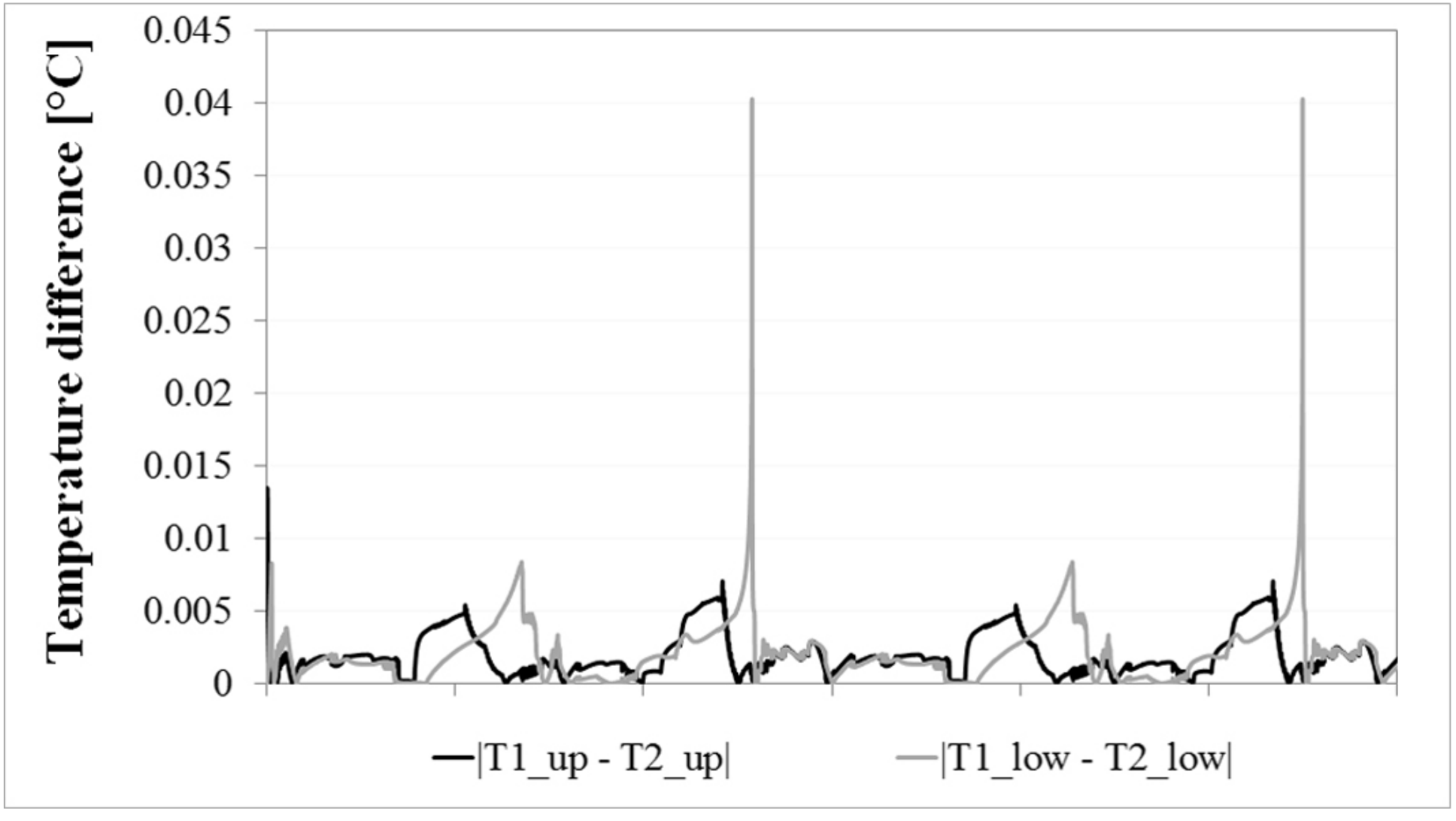
Temperature difference [°C]
0.045
0.04
0.035
0.03
0.025
0.02
0.015
0.01
0.005
0
|T1_up - T2_up|
|T1_low - T2_low|

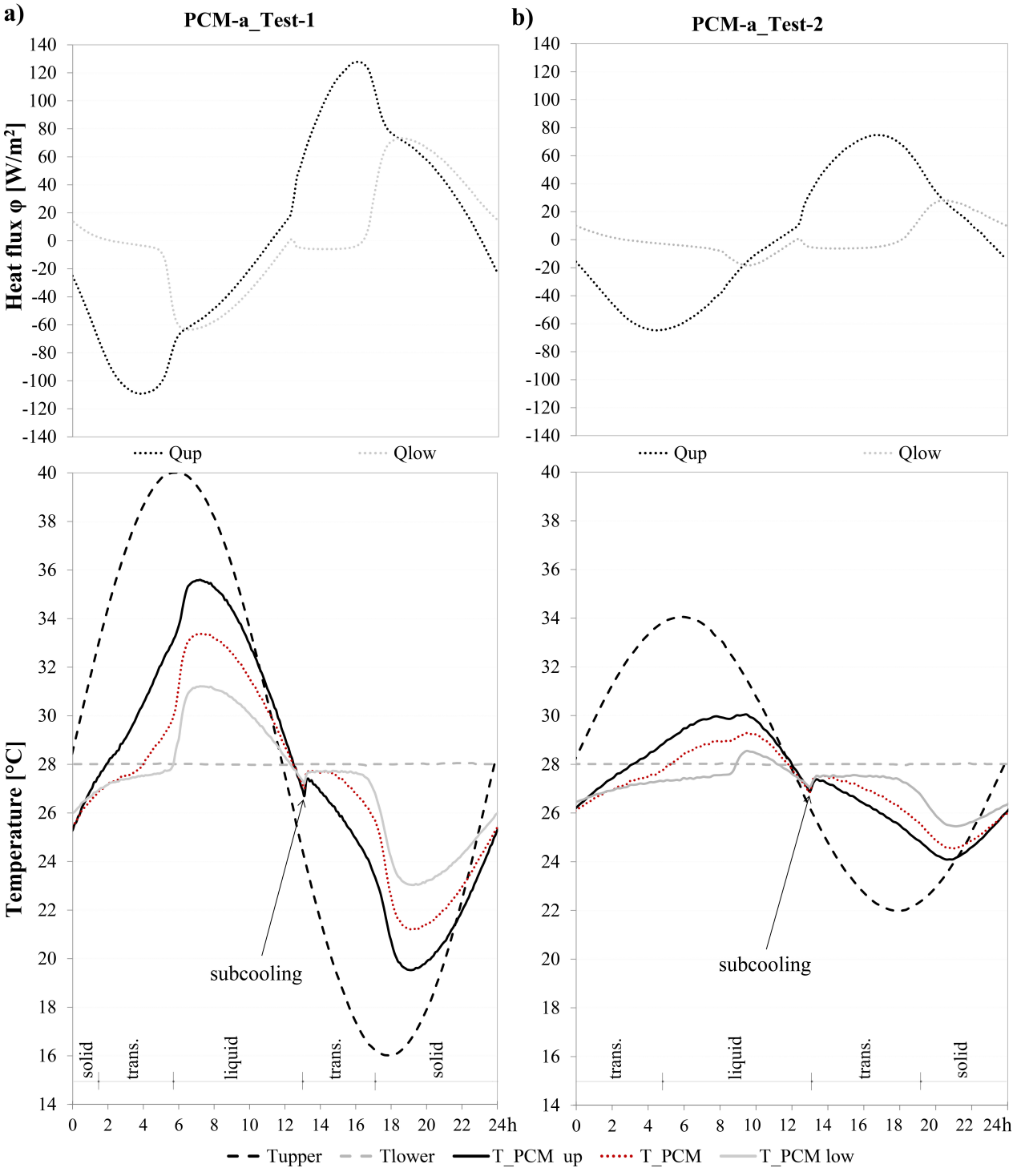
a)
PCM-a_Test-1
b)
PCM-a_Test-2
Heat flux φ [W/m²]
Qup
Qlow
Temperature [°C]
subcooling
solid
trans.
liquid
trans.
solid
Tupper
Tlower
T_PCM up
T_PCM
T_PCM low
24h

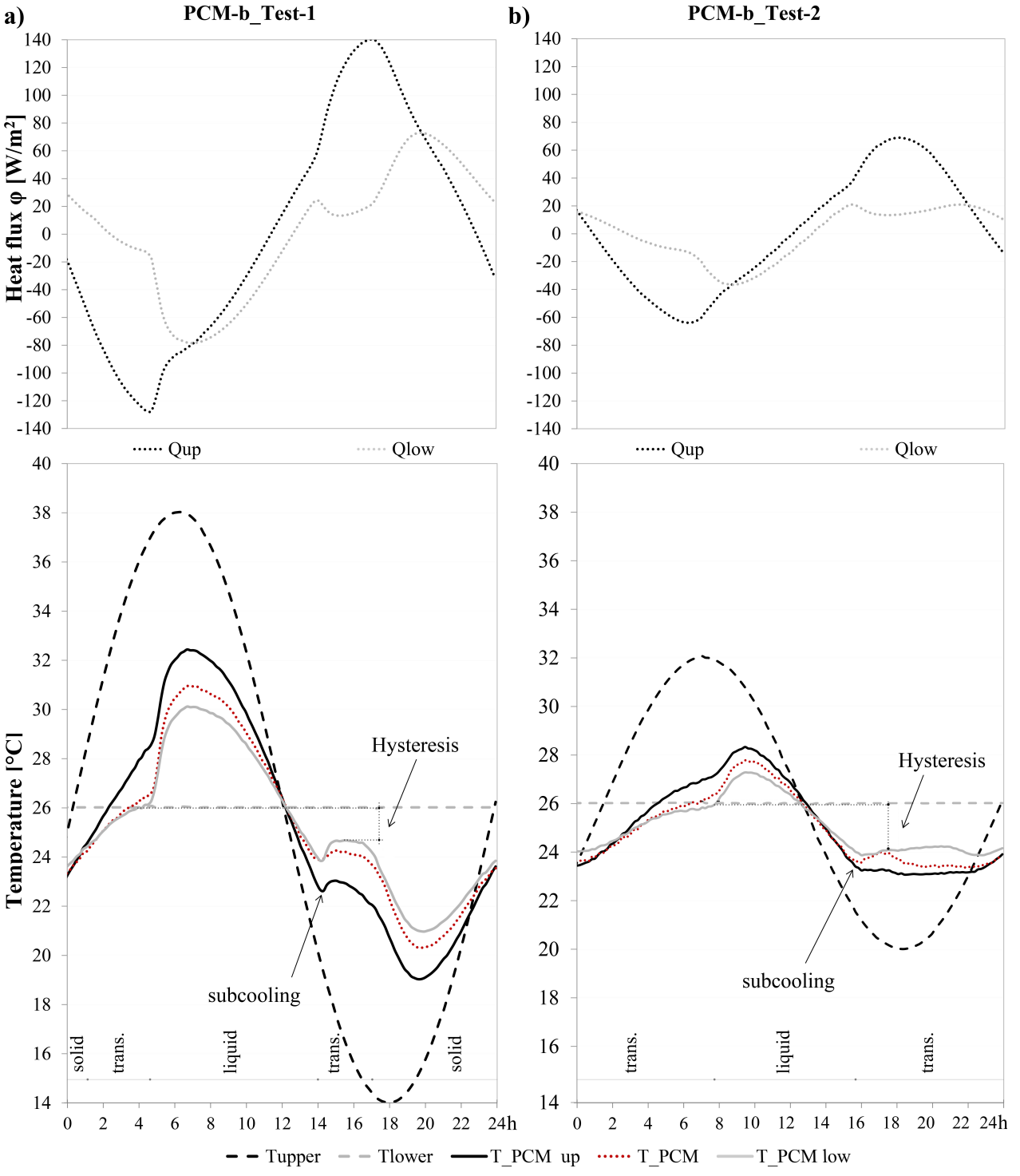
a)
PCM-b_Test-1
b)
PCM-b_Test-2
Heat flux φ [W/m²]
Qup
Qlow
Temperature [°C]
Hysteresis
subcooling
solid
trans.
liquid
trans.
solid
Tupper
Tlower
T_PCM up
T_PCM
T_PCM low
0 2 4 6 8 10 12 14 16 18 20 22 24h

List of tables and correspondent captions

Table 1. Thermophysical properties of the two PCMs **Error! Reference source not found.** – Nominal values.

name	commercial name	material class	melting range	congealing range	c	Latent heat storage capacity	ρ (solid)	ρ (liquid)	λ (both phases)
			[°C]	[°C]	[kJ/(kg·K)]	[kJ/kg]	[kg/m³]	[kg/m³]	[W/(m·K)]
PCM-a	RT 28 HC	Paraffin Wax	27-29	29-27	2	216[a]	880	770	0.200
PCM-b	SP 26 E	Salt Hydrate	25-27	25-24	2	153[b]	1500	1400	0.600

[a] Latent heat capacity over a 26-29°C temperature range (average values between the latent heat of fusion and solidification)
[b] Latent heat capacity over a 23-26°C temperature range (average values between the latent heat of fusion and solidification)

Table 2. Physical properties of each material that constitutes the specimen **Error! Reference source not found.**.

layer	material	d [mm]	ρ [kg/m³]	c [kJ/(kg·K)]	λ [W/(mK)]
1	Gypsum board	12.5	720	1.09	0.190
2	Polycarbonate	0.5	1200	1.20	0.205
3	PCM layer*	9.0	-	-	-
4	Polycarbonate	0.5	1200	1.20	0.205
5	Gypsum board	12.5	720	1.09	0.190

* The PCM properties are reported in Table 1.

Table 3. Thermal conductivity λ, (T_{upper}, T_{lower}, are the upper plate and the lower plate temperatures, respectively)

Specimen/type	Test	Heat flux direction	T_{up} [°C]	T_{low} [°C]	$\lambda_{declared}$ [W/mK]	$\lambda_{eq,\ measured}$ [W/mK]
PCM-a - Organic (paraffin wax)	Test 1 (solid)	upward	15	25	0.20	0.29±0.04
		downward	25	15		0.28±0.04
	Test 2 (liquid)	upward	30	40		0.41±0.07
		downward	40	30		0.15±0.01
PCM-b - Inorganic (salt hydrate)	Test 1 (solid)	upward	15	25	0.60	0.59±0.11
		downward	25	15		0.59±0.11
	Test 2 (liquid)	upward	30	40		0.46±0.07
		downward	40	30		0.45±0.06

Authors' declaration.

Conflicts of interest: none